Korean J Physiol Pharmacol 2023;27(3):209-220
https://doi.org/10.4196/kjpp.2023.27.3.209

KJPP

Original Article

# Edaravone alleviates lung damage in mice with hypoxic pulmonary hypertension by increasing nitric oxide synthase 3 expression

Wan Zheng*, Tianfa Li, Junping Wei, Yani Yan, and Shanshan Yang

*Department of Cardiovascular Medicine, The First Affiliated Hospital of Hainan Medical University, Haikou, Hainan 570102, P.R. China*

**ARTICLE INFO**

**Received** June 8, 2022
**Revised** August 2, 2022
**Accepted** August 2, 2022

***Correspondence**
Wan Zheng
E-mail: meol263@163.com

**Key Words**
Edaravone
Hypertension, pulmonary
Lung injury
Nitric oxide synthase

**ABSTRACT** This study is to determine the regulation of nitric oxide synthase 3 (NOS3) by edaravone in mice with hypoxic pulmonary hypertension (HPH). C57BL/6J mice were reared in a hypoxic chamber. HPH mice were treated with edaravone or edaravone + L-NMMA (a NOS inhibitor). Lung tissue was collected for histological assessment, apoptosis analysis, and detection of malondialdehyde, superoxide dismutase, tumor necrosis factor (TNF)-α, interleukin (IL)-6, and NOS3. The levels of serum TNF-α and IL-6 were also measured. Immunohistochemistry was used to visualize the expression of α-smooth muscle actin (SMA) in pulmonary arterioles. Edaravone treatment improved hemodynamics, inhibited right ventricular hypertrophy, increased NOS3 expression, and reduced pathological changes, pulmonary artery wall thickness, apoptotic pulmonary cells, oxidative stress, and the expression of TNF-α, IL-6, and α-SMA in HPH mice. L-NMMA treatment counteracted the lung protective effects of edaravone. In conclusion, edaravone might reduce lung damage in HPH mice by increasing the expression of NOS3.

## INTRODUCTION

Pulmonary hypertension is defined as an abnormal hemodynamic state with a mean pulmonary arterial pressure (mPAP) of or above 20 mmHg at rest, which can be caused by left-sided heart disease, chronic lung disease and/or hypoxia, pulmonary embolism, and other unclear factors [1]. Pulmonary hypertension affects about 1% of the global population, especially in elderly people and individuals with heart failure, and independently predicts clinical deterioration and increased mortality [2]. Sustained exposure to hypoxia gives rise to pulmonary vascular remodeling and constriction and consequently leads to hypoxic pulmonary hypertension (HPH) that imposes an increased workload on the right ventricle (RV) [3].

Edaravone is an antioxidant drug newly approved by the Food and Drug Administration for the treatment of amyotrophic lateral sclerosis (ALS) [4]. Edaravone effectively suppresses the deterioration of motor neurons by protecting against free radicals in the early stages of ALS [5]. Edaravone scavenges multiple free radicals by moving an electron from its anionic form to radicals and transforming itself into a butanoic acid [6]. As a free radical scavenger, edaravone reduced the secretion of pro-inflammatory cytokines from alveolar macrophages in lipopolysaccharide (LPS)-induced acute lung injury (ALI) [7]. Edaravone could also restrain pulmonary hypertension in neonatal sepsis by reducing the level of tumor necrosis factor (TNF)-α [8]. However, whether edaravone imposes inhibitory effects on pulmonary hypertension under hypoxic conditions remains unknown.

Nitric oxide synthase (NOS) is a class of enzymes that catalyze the production of nitric oxide (NO) and has three isoforms with distinct functions [9]. NOS3 is specifically expressed in the vascular endothelium where it regulates vascular tone and remodeling,



**Author contributions:** W.Z. conceived the ideas. W.Z. and T.F.L. designed the experiments. W.Z., T.F.L., and J.P.W. performed the experiments. W.Z., T.F.L., and Y.N.Y. analyzed the data. W.Z. and T.F.L. provided critical materials. W.Z. and S.S.Y. wrote the manuscript. All the authors have read and approved the final version for publication.

homeostasis, angiogenesis, and progenitor cell mobilization [10]. A basal level of NO generated by NOS3 not only controls blood flow but suppresses platelet activation and adherence of inflammatory leukocytes to the blood vessel wall [11]. Dysregulation of the NO pathway in the pulmonary endothelium contributes to the initiation and progression of pulmonary arterial hypertension by promoting vascular smooth muscle tone and vascular remodeling [12]. Chalupsky and colleagues [13] detected uncoupled NOS3 along with decreased NO bioavailability in human pulmonary artery endothelial cells and murine pulmonary arteries under hypoxic conditions.

From the above evidence, NOS3 plays an essential role in maintaining the normal pulmonary vascular function and edaravone may protect against pulmonary hypertension by regulating the expression of NOS3. This study was designed to analyze the action mechanism of edaravone in HPH and provide new strategies for HPH treatment.

# METHODS

## Experimental animals

Seventy male C57BL/6J mice (20 ± 2 g) were purchased from Beijing Vital River Laboratory Animal Technology Co., Ltd. and housed in a specific pathogen-free animal room. The room temperature and relative humidity were maintained at 21°C–25°C and 50%–65%, respectively. The mice were subjected to 12-h shifts of light-dark cycles and given free access to water and food. Experiments were carried out after the mice were fed for one week. The protocols of the animal experiments were approved by the Ethics Committee of The First Affiliated Hospital of Hainan Medical University.

## HPH mouse model

An HPH mouse model was established using the methods of Eddahibi and colleagues [14]. C57BL/6J mice were placed in a self-made, full-automatic normobaric hypoxic chamber and inhaled 10% nitrogen-oxygen gases delivered at 1.5 L/min. The concentration of oxygen was monitored and maintained within 9.5%–10.5%. The pressure was adjusted through a pressure reducing valve and a solenoid valve. Water vapor and carbon dioxide in the chamber were absorbed by anhydrous calcium chloride and soda lime. The hypoxia lasted for 24 h every day.

## Animal grouping and treatment

The 70 C57BL/6J mice were divided into control, HPH, edaravone (low-dose, medium-dose, and high-dose), edaravone + saline, and edaravone + L-NMMA groups (10 animals per group). The control group was housed in a normal environment and the remaining groups were kept in a normobaric and hypoxic environment for 8 weeks. After the model establishment, the mice were reared in the normobaric and hypoxic environment for 2 weeks, during which the HPH group was untreated and the edaravone groups were injected with low-dose (1 mg/kg), medium-dose (5 mg/kg), or high-dose (10 mg/kg) edaravone through the tail vein every day. In addition to treatment with 5 mg/kg edaravone, the edaravone + L-NMMA group was given an intraperitoneal injection of 40 mg/kg NOS inhibitor L-NMMA [15] every day and the edaravone + saline group were injected with an equal amount of normal saline.

## Measurements of cardiovascular function and cardiac structure

Mice were anesthetized with 1% sodium pentobarbital (40 mg/kg, intraperitoneal injection) and fixed in supine positions. After disinfection, the neck was incised in the middle and the subcutaneous tissues and muscles were bluntly separated. A polyethylene hose filled with heparin saline was slowly inserted into the RV through the right internal jugular vein and right atrium. The other end of the hose was connected to an electrocardiogram monitoring system through a pressure transducer. The right ventricular systolic pressure (RVSP) and mPAP were recorded in real time and averaged.

The mice were sacrificed immediately after the pressure measurement and their hearts were taken out and fixed in formaldehyde at room temperature for 48 h. The RV, left ventricle (LV), and ventricular septum (S) were separated and weighed. The RV hypertrophy index [RV / (LV + S)] was calculated to evaluate RV remodeling.

## Collection of serum and lung tissue

Blood and lung tissue were collected at the 10th week. Blood taken from the orbit was stored at room temperature for 30 min and centrifuged at 3,000 r/min, 4°C for 15 min. The serum was aliquoted and stored at −80°C. Next, the mice were sacrificed for collection of lung tissue.

## Hematoxylin-eosin (H&E) staining

Lung tissue was fixed in 4% paraformaldehyde for 48 h and made into paraffin sections (4 μm). Hydrated tissue slices were sequentially immersed in the following solutions: hematoxylin solution (3–5 min), ionized water, 1% hydrochloric acid-ethanol (20 sec), 1% ammonia (30 sec), ionized water, 1% eosin solution (5 min), running water (5 min), ionized water (1 min), 75% ethanol (5 min), 90% ethanol (5 min), 95% ethanol (5 min), absolute ethanol (5 min), and xylene (2 × 10 min). The thickness of the anterior artery wall was calculated using the following formula: wall thickness (WT%) = (wall thickness / outer diameter) × 100%.

## Immunohistochemistry (IHC)

Hydrated lung tissue slices sequentially underwent 3% $H_2O_2$ treatment at room temperature for 10 min, heat-induced antigen retrieval, and normal goat serum treatment at room temperature for 20 min (excess liquid was shaken off). The slices were washed thrice with phosphate-buffered saline before each step. Anti-α-smooth muscle actin (SMA) (56856S; Cell Signaling Technology) was added dropwise to the slices and incubated overnight at 4°C. A secondary antibody was incubated with the slices at room temperature for 1 h. After treatment with 3,3′-diaminobenzidine (DAB) for 1–3 min, the slices were immersed in hematoxylin solution for 3 min, dehydrated, and transparentized. The slices were observed under a microscope (×200). Three fields of view were randomly selected and imported into the Image J software for semi-quantitative analysis. The percentage of positive cells was scored as follows: < 5% = 0 point, 5%–25% = 1 point, 26%–50% = 2 points, 51%–75% = 3 points, 76%–100% = 4 points. The scoring criteria for the intensity of positive staining were: colorless = 0 point, pale yellow = 1 point, brown-yellow = 2 points, tan = 3 points. The final positive degree was expressed as the multiplication of the two scores: 0 was negative, 1–4 was weakly positive, 5-8 was positive, and 9–12 was strongly positive.

## Terminal dUTP nick-end labeling (TUNEL) staining

Mouse lung tissue was fixed in 4% paraformaldehyde overnight and embedded in paraffin. The embedded tissue was sliced, from which 5 slices were taken. After dewaxing and hydration, each slice was incubated with 50 μl of 1% proteinase K solution at 37°C for 30 min and then with methanol solution containing 0.3% $H_2O_2$ (for eliminating the activity of endogenous peroxidases) at 37°C for 30 min, followed by sequential incubation with the TUNEL reaction solution, terminal deoxynucleotidyl transferase, and horseradish enzyme-labeled streptavidin. After 2% DAB treatment for 15 min at room temperature and nuclei counterstaining with hematoxylin, the slices were dehydrated, cleared, mounted with neutral gum, and observed under a microscope (Olympus).

## ELISA

The expression of interleukin (IL)-6 and TNF-α in serum and lung tissue was detected using a IL-6 ELISA kit (ab222503; Abcam) and a TNF-α ELISA kit (ab208348; Abcam).

## Detection of NO

The contents of NO in lung tissue were measured using a total NO detection kit (Beyotime) based on the Griess method.

## Detection of malondialdehyde (MDA) and superoxide dismutase (SOD)

The levels of the oxidative stress markers MDA and SOD were measured using a SOD kit (S0101S; Beyotime) and a MDA kit (S0131S; Beyotime).

## Quantitative reverse transcription polymerase chain reaction (qRT-PCR)

TRIzol reagent was used for extraction of total RNA from lung tissue. RNA purity and concentration were measured by a NanoDrop analyzer. A reverse transcription kit (Takara) was used for synthesis of cDNA. SYBR Green Mix (Takara) was used for qRT-PCR that was performed on the Applied Biosystems 7300 Real-Time PCR System (ABI). Each sample had three duplicates. The $2^{-\Delta\Delta Ct}$ method [16] was adopted for data analysis. $\Delta\Delta Ct = (Ct_{\text{target gene}} - Ct_{\text{internal reference}})_{\text{experimental group}} - (Ct_{\text{target gene}} - Ct_{\text{internal reference}})_{\text{control group}}$. β-Actin was used as the reference gene. See Table 1 for the information of used primers.

## Western blotting

Lung tissue was lysed with RIPA buffer (Beyotime), on ice, for 15 min and centrifuged at 13,000 g for 5 min, followed by measurement of concentrations of protein samples using a bicinchoninic acid kit (Beyotime). The protein samples were added into loading buffer and denatured in boiling water for 10 min. The loading volume of each sample was calculated using a constant amount. The samples were electrophoresed on gels at 80 V for 30 min and after bromophenol blue entered the separation gel, the electrophoresis was run at 120 V for 90 min. Separated proteins of each group were transferred onto a PVDF membrane in an ice bath (250 mA, 100 min). The membrane was washed thrice (1–2 min each time) and placed in blocking solution for 2 h before incubation with antibodies against NOS3 (1:1,000, ab76198; Abcam) and β-actin (1:1,000, 4970S; Cell Signaling) at 4°C overnight. The membrane was incubated with a secondary antibody (HRP-labeled goat anti-rabbit IgG; 1:1,000, A0208; Beyotime) at room temperature for 2 h. Finally, the membrane was treated with ECL color developing solution (P0018FS; Beyotime) and images were captured by a chemiluminescence imaging system (Bio-rad).

**Table 1. Primer sequences**

| Name of primer | Sequences (5′ to 3′) |
|---|---|
| NOS3-F | AATCTTGAAGGTTCCTCCGGC |
| NOS3-R | TCTGGGACTCACTGTCAAAGA |
| β-actin-F | TGTACCCAGGCATTGCTGAC |
| β-actin-R | AACGCAGCTCAGTAACAGTCC |

NOS3, nitric oxide synthase 3; F, forward primer; R, reverse primer.

### Statistical analysis

Data were analyzed using GraphPad Prism 7 (GraphPad Software Inc.). All data were expressed as mean ± standard deviation. T-test was used for comparisons between two groups and one-way analysis of variance for comparisons among multiple groups. Tukey's test was used for *post-hoc* multiple comparisons. Significant differences were represented by $p < 0.05$.

## RESULTS

### Establishment of an HPH mouse model

First, we established an HPH mouse model using continuous hypoxia exposure and validated it through the following experiments. The pathological images revealed by H&E staining showed that in the HPH group, the lung microvessels were dilated and congested, the lungs were enlarged, and the alveolar septum was thickened; there were also pulmonary edema, leakage of red blood cells and fluid from the alveolar cavity and septum, inflammatory cell infiltration, and alveoli of various sizes in this group (Fig. 1A). Additionally, through analysis of the H&E images, we found the wall of pulmonary arterioles was thickened and WT (%) increased significantly in the HPH group (Fig. 1A, $^{**}p < 0.01$). The hemodynamic parameters RVSP (Fig. 1B, $^{*}p < 0.05$) and mPAP (Fig. 1C, $^{**}p < 0.01$) rose in the model group. The value of RV / (LV + S) was also elevated in the model group (Fig. 1D, $^{**}p < 0.01$), suggesting an increase in the degree of RV hypertrophy.

### HPH exacerbates pulmonary damage

Next, we evaluated pulmonary damage in HPH mice. Pulmonary cell apoptosis was observed using TUNEL staining. The images showed that the model group had a larger number of TUNEL-positive cells than the control group (Fig. 2A). ELISA was performed to detect the inflammatory factors TNF-α and IL-6 in serum and lung tissue. The analysis showed that the model group had higher expression levels of TNF-α and IL-6 than the control group (Fig. 2B, $^{***}p < 0.001$). The expression of MDA increased while that of SOD decreased in the model group (Fig. 2C, $^{*}p < 0.05$). IHC was used to visualize the expression of α-SMA in pulmonary arteriole tissue. The results showed that α-SMA was upregulated in the model group, compared with that in the control group (Fig. 2D, $^{*}p < 0.05$), indicating an increase in the degree of pulmonary fibrosis. The above results suggest that the lung damage in HPH mice is aggravated.

### Edaravone reduces pulmonary injury in HPH mice

First, we explored the effects of different doses of edaravone on pulmonary injury in HPH mice. The H&E images showed that 5 or 10 mg/kg edaravone treatment alleviated alveolar leakage, dilation and congestion of capillaries, and inflammatory cell

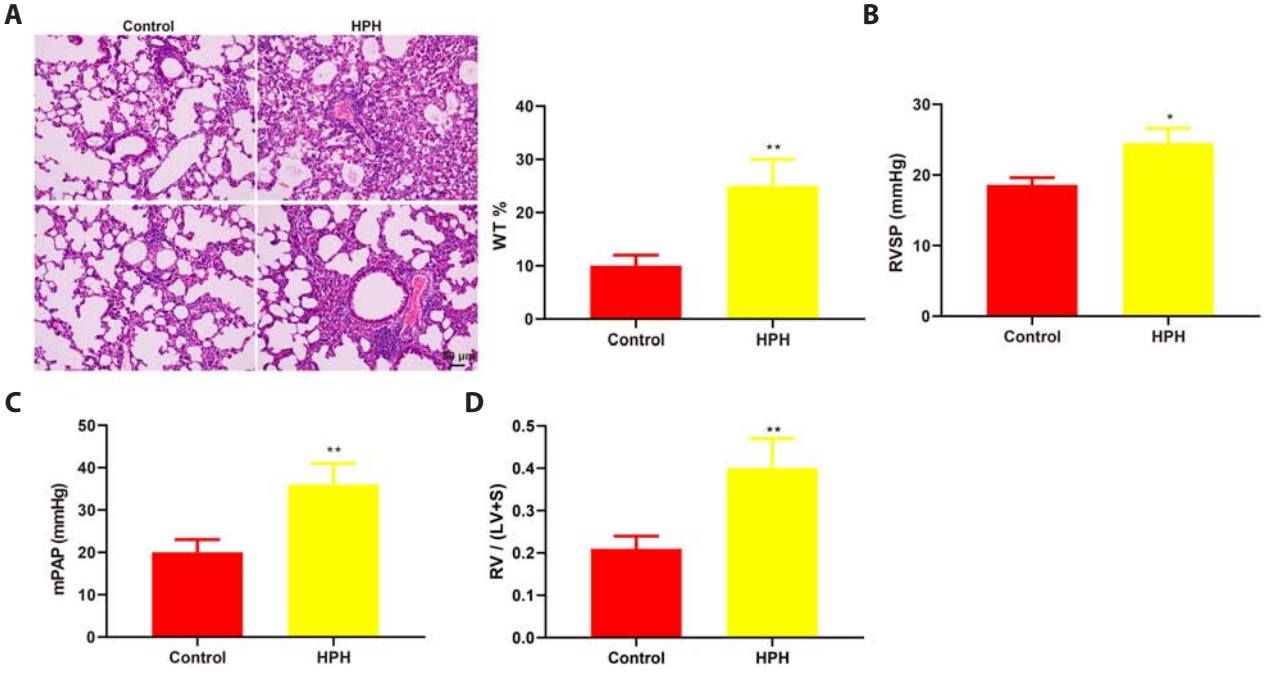


**Fig. 1. Establishment of an HPH mouse model.** (A) H&E staining was used to reveal the pathological changes of lung tissue and the remodeling of pulmonary vessels (×200). RVSP (B), mPAP (C), and RV / (LV + S) (D) were measured. The data were expressed as mean ± SD. n = 10. HPH, hypoxic pulmonary hypertension; WT, wall thickness; RVSP, right ventricular systolic pressure; mPAP, mean pulmonary artery pressure; RV, right ventricle; LV, left ventricle; S, septum. $^{*}p < 0.05$ and $^{**}p < 0.01$, compared with the control group.

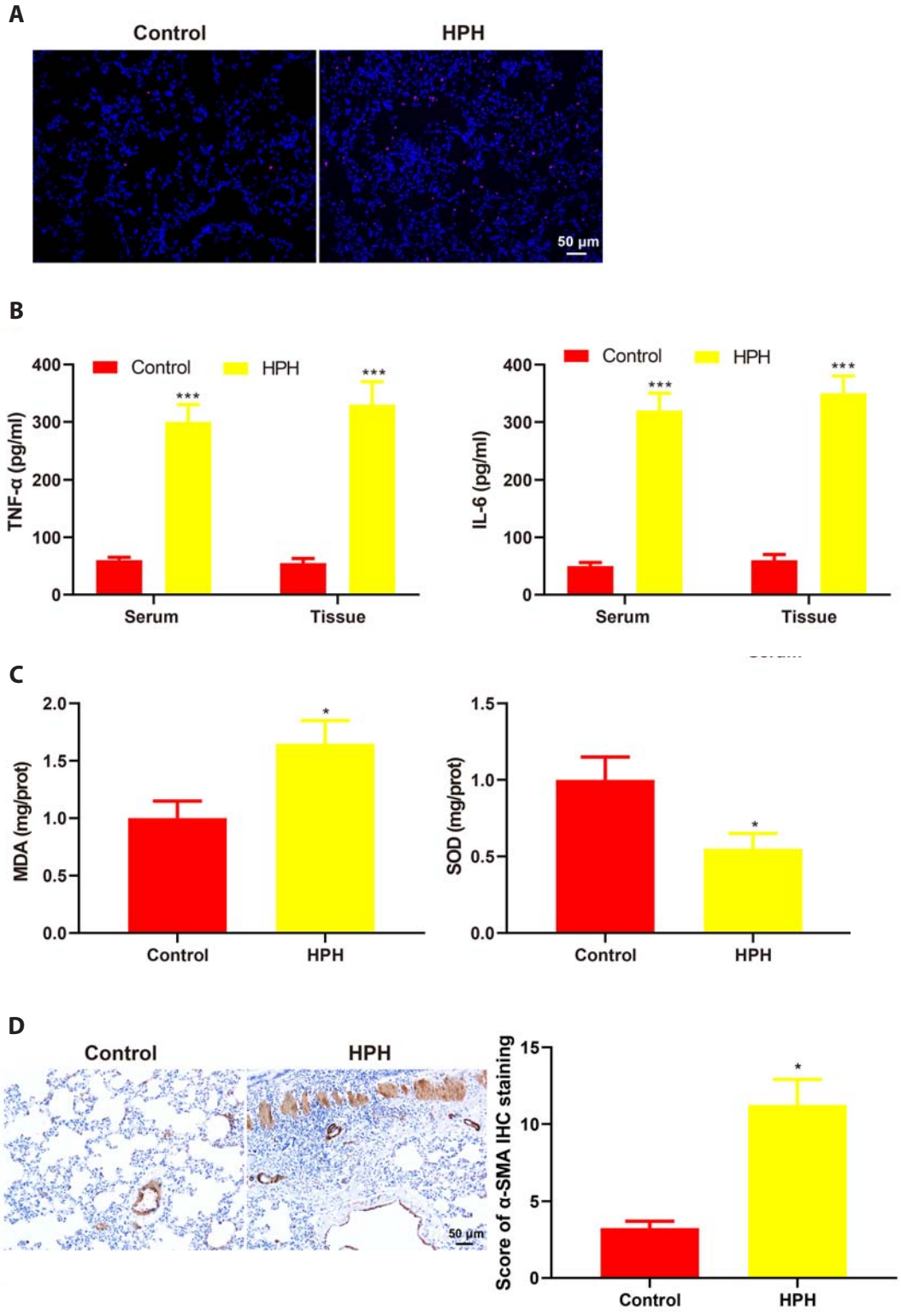


**Fig. 2. HPH exacerbates pulmonary damage.** (A) Terminal deoxynucleotidyl transferase dUTP nick end labeling was used to reveal pulmonary cell apoptosis (×200). (B) Enzyme-linked immunosorbent assay was performed to detect the expression of TNF-α and IL-6 in serum and lung tissue. (C) The expression of MAD and SOD was measured. (D) Immunohistochemistry was used to reveal the expression of α-SMA in pulmonary arterioles (×200). The data were expressed as mean ± SD. n = 10. HPH, hypoxic pulmonary hypertension; TNF, tumor necrosis factor; IL, interleukin; MAD, malondialdehyde; SOD, superoxide dismutase; α-SMA, α-smooth muscle actin. *$p < 0.05$ and ***$p < 0.001$, compared with the control group.

infiltration in the lung tissue of HPH mice (Fig. 3A). Moreover, 5 or 10 mg/kg edaravone treatment reduced WT% (Fig. 3A, $^{\#\#}p < 0.01$), TUNEL-positive cells in the lung tissue (Fig. 3A), and the values of RVSP, mPAP, and RV / (LV + S) (Fig. 3B, C, $^{\#}p < 0.05$). The results of ELISA showed that 5 or 10 mg/kg edaravone treatment decreased the levels of TNF-α and IL-6 in the serum and lung tissue of HPH mice (Fig. 3D, E, $^{\#\#}p < 0.01$). The expression of MDA declined and that of SOD increased after 5 or 10 mg/kg edaravone treatment (Fig. 3F, $^{\#}p < 0.05$). IHC analysis showed that 5 or 10 mg/kg edaravone treatment inhibited the expression of α-SMA in the pulmonary arterioles of HPH mice (Fig. 3G, $^{\#}p < 0.05$). Of note, there were no significant differences in the above

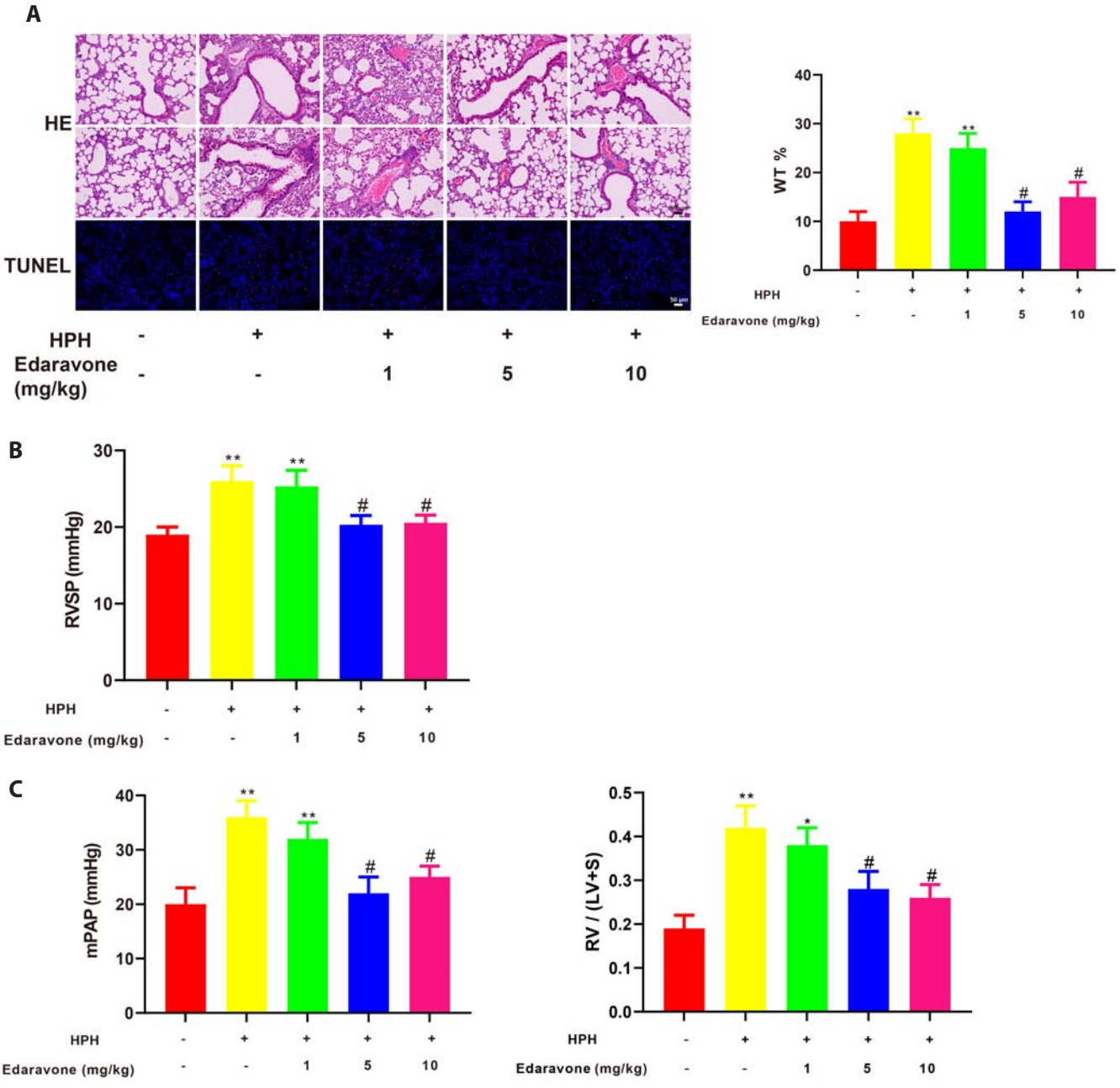


**Fig. 3. Edaravone reduces pulmonary injury in HPH mice.** (A) H&E staining was used to reveal the pathological changes of lung tissue and the remodeling of pulmonary vessels (×200); terminal deoxynucleotidyl transferase dUTP nick end labeling was used to reveal pulmonary cell apoptosis (×200). (B, C) RVSP, mPAP, and RV / (LV + S) were measured. Enzyme-linked immunosorbent assay was performed to detect the expression of TNF-α (D) and IL-6 (E) in serum and lung tissue. (F) The expression of MAD and SOD was measured. (G) Immunohistochemistry was used to reveal the expression of α-SMA in pulmonary arterioles (×200). The data were expressed as mean ± SD. n = 10. HPH, hypoxic pulmonary hypertension; WT, wall thickness; RVSP, right ventricular systolic pressure; mPAP, mean pulmonary artery pressure; RV, right ventricle; LV, left ventricle; S, septum; TNF, tumor necrosis factor; IL, interleukin; MAD, malondialdehyde; SOD, superoxide dismutase; α-SMA, α-smooth muscle actin. *p < 0.05, **p < 0.01, and ***p < 0.001, compared with the control group. $^{\#}p < 0.05$ and $^{\#\#}p < 0.01$, compared with the HPH group.

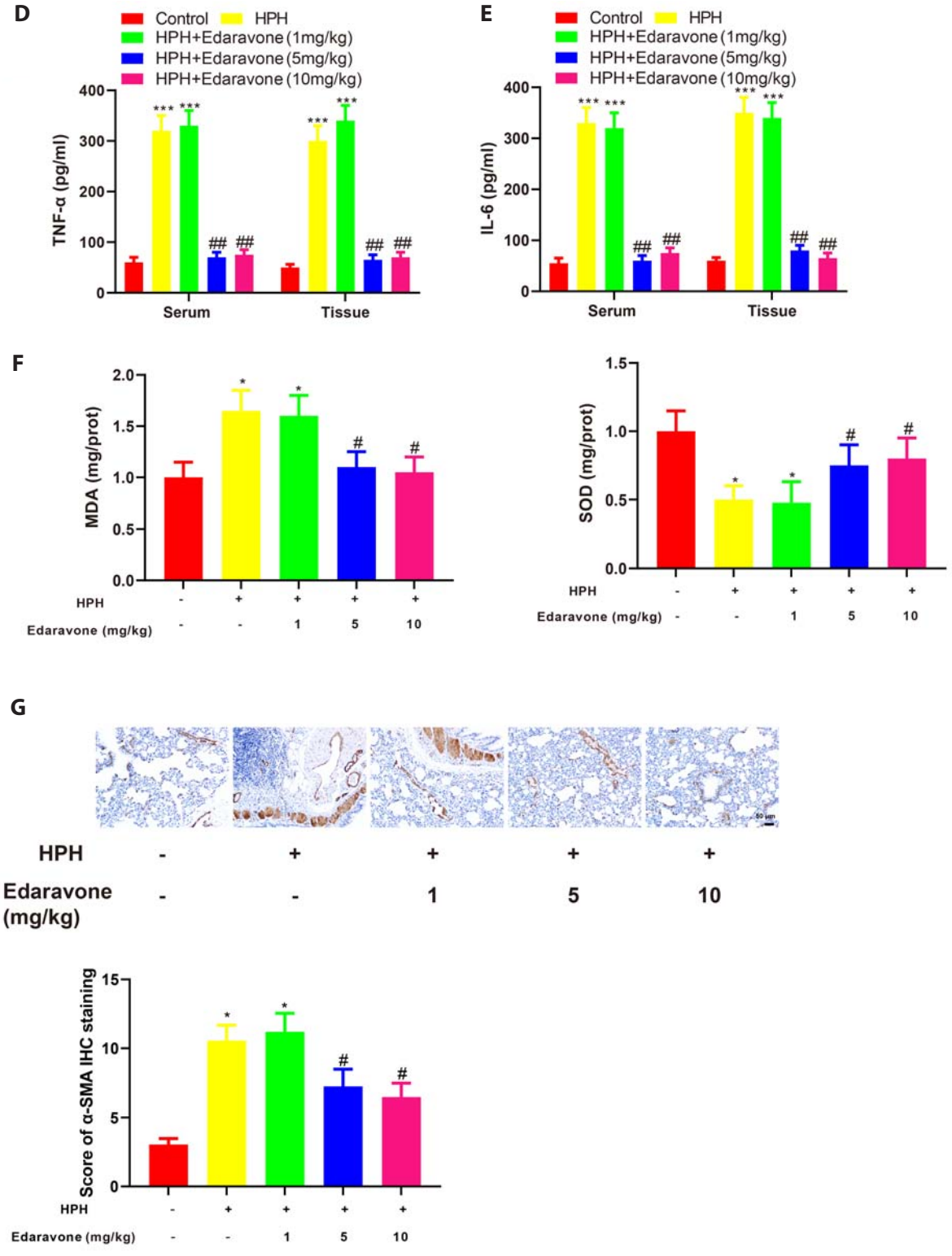


**Fig. 3.** Continued.

experiment results between the 5 mg/kg edaravone and 10 mg/kg edaravone groups or between the HPH and 1 mg/kg edaravone groups (Fig. 3A–G, $p > 0.05$). Therefore, the dose of edaravone was set at 5 mg/kg in the following experiments. Altogether, these results indicate that edaravone can reduce pulmonary injury in HPH mice.

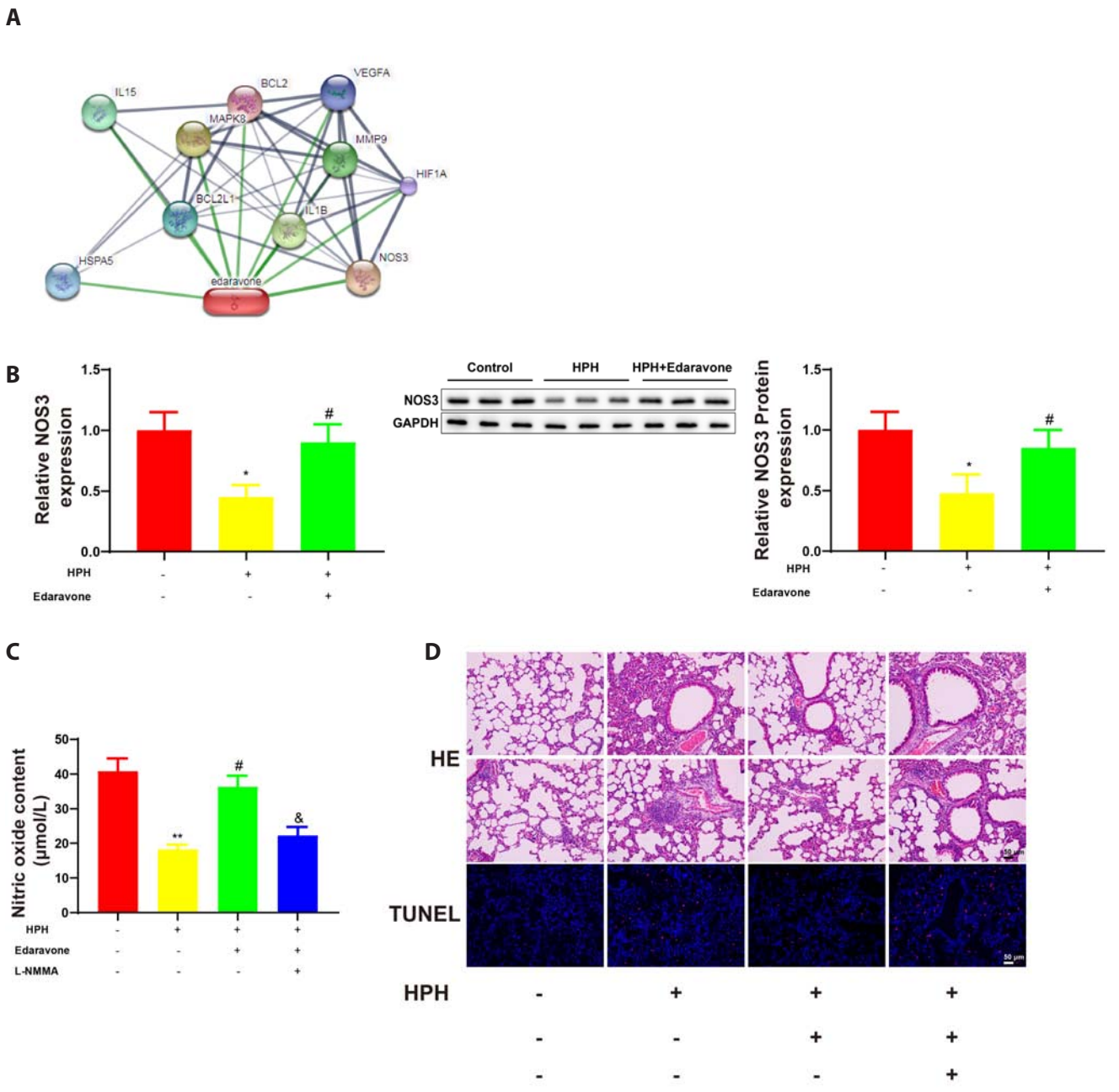


**Fig. 4. Edaravone alleviates pulmonary damage in HPH mice by targeting NOS3.** (A) STITCH analyzed the target proteins of edaravone. (B) Quantitative reverse transcription polymerase chain reaction and western blotting were used to detect the expression of NOS3 mRNA and protein in the lung tissue of HPH mice before and after edaravone treatment. Next, HPH mice were injected with 5 mg/kg edaravone and 40 mg/kg NOS inhibitor L-NMMA. (C) The Griess method was used for detecting the contents of NO in lung tissue. (D) H&E staining was used to reveal the pathological changes of lung tissue and the remodeling of pulmonary vessels (×200); terminal deoxynucleotidyl transferase dUTP nick end labeling was used to reveal pulmonary cell apoptosis (×200). (E, F) WT, RVSP, mPAP, and RV / (LV + S) were measured. (G) Enzyme-linked immunosorbent assay was performed to detect the expression of TNF-α and IL-6 in serum and lung tissue. (H) The expression of MAD and SOD was measured. (I) Immunohistochemistry was used to reveal the expression of α-SMA in pulmonary arterioles (×200). The data were expressed as mean ± SD. n = 10. HPH, hypoxic pulmonary hypertension; NOS3, nitric oxide synthase 3; NO, nitric oxide; WT, wall thickness; RVSP, right ventricular systolic pressure; mPAP, mean pulmonary artery pressure; RV, right ventricle; LV, left ventricle; S, septum; TNF, tumor necrosis factor; IL, interleukin; MAD, malondialdehyde; SOD, superoxide dismutase; α-SMA, α-smooth muscle actin. *$p < 0.05$, **$p < 0.01$, and ***$p < 0.001$, compared with the control group. $^{\#}p < 0.05$, $^{\#\#}p < 0.01$, and $^{\#\#\#}p < 0.001$, compared with the HPH group. $^{\&}p < 0.05$, $^{\&\&}p < 0.01$, and $^{\&\&\&}p < 0.001$, compared with the HPH + edaravone group.

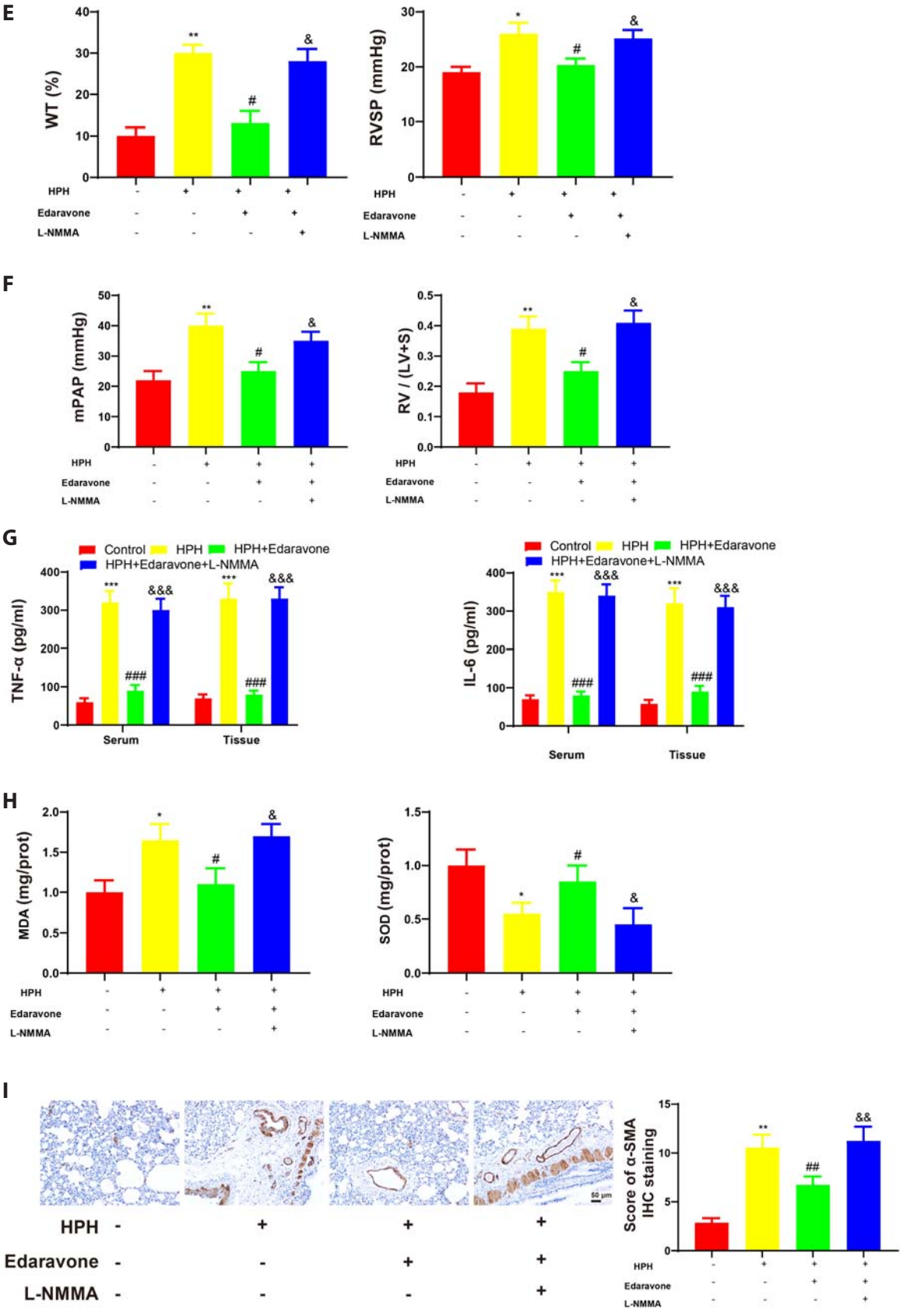


**Fig. 4.** Continued.

### Edaravone alleviates pulmonary damage in HPH mice by increasing NOS3 expression

To analyze the action mechanism of edaravone, we used the STITCH website (http://stitch.embl.de) to predict the target proteins of edaravone and found there was an interaction between edaravone and NOS3 (Fig. 4A). NOS3 was downregulated in the lung tissue of HPH mice (*$p < 0.05$); however, the expression of NOS3 mRNA and protein was increased by edaravone treatment ($^{\#}p < 0.05$) (Fig. 4B). To determine the regulation of NOS3 by edaravone in HPH, we injected HPH mice with 5 mg/kg edaravone and 40 mg/kg NOS inhibitor L-NMMA. The contents of NO in lung tissue were detected to determine the effect of L-NMMA on NOS3 activity. HPH mice showed significantly lower contents of NO than control mice (**$p < 0.01$); however, the NO contents in HPH mice were increased by edaravone treatment ($^{\#}p < 0.05$). It was notable that L-NMMA reversed edaravone-induced increase in NO contents in HPH mice (Fig. 4C, $^{\&}p < 0.05$). The results of histological staining showed that L-NMMA treatment increased alveolar leakage, dilation and congestion of capillaries, inflammatory cell infiltration, and TUNEL-positive cells in the lung tissue of edaravone-treated HPH mice (Fig. 4D). Compared with the edaravone group, the edaravone + L-NMMA group showed higher WT%, RVSP, mPAP, and RV / (LV + S) (Fig. 4E, F, $^{\&}p < 0.05$), increased expression of TNF-α, IL-6, MDA, and α-SMA (Fig. 4G, $^{\&\&\&}p < 0.001$; Fig. 4H, $^{\&}p < 0.05$; Fig. 4I, $^{\&\&}p < 0.01$), and decreased expression of SOD (Fig. 4H, $^{\&}p < 0.05$). Collectively, these data indicate that edaravone alleviates pulmonary damage in HPH mice by increasing the expression of NOS3.

## DISCUSSION

Pulmonary hypertension is a term embracing various disease forms that differ widely in incidence, clinical significance, and treatment [17]. Lung disease and/or hypoxia rank the second leading causes of pulmonary hypertension; however, HPH could not be effectively managed with the currently approved drugs for pulmonary arterial hypertension, which calls for a better understanding of the disease mechanisms and development of new therapies [18]. This study used continuous hypoxia exposure to induce HPH in C57BL/6J mice and detected exacerbated lung injury in HPH mice. An antioxidant drug, edaravone, effectively protected mice against HPH-induced lung injury. Through bioinformatics analysis and experimental validation, edaravone was found to exert lung protective effects in HPH mice by regulating the expression of NOS3.

Edaravone is a free radical scavenger that possesses combined properties of vitamin C and D in preventing free radical-induced peroxidation in both the lipid and aqueous phases [19]. Edaravone reduces oxidative damage and cell apoptosis in models of retinal diseases, spinal cord injury, ischemic cerebral injury, and chronic renal injury [20-24]. The therapeutic effects of edaravone have also been proven in lung injury under various conditions. For example, pretreatment with edaravone alleviated lung injury post hind limb ischemia/reperfusion by reducing oxidative stress and inflammation [25]. Apart from oxidative stress, edaravone pretreatment imposes inhibition on necroptosis in hyperoxic ALI [26]. Edaravone combined with dexamethasone restored mitochondrial function and inhibited apoptosis in the lungs of rats exposed to smoke [27]. Xiao and colleagues [28,29] found that edaravone might suppress smoke-induced inhalational lung injury by blocking the Notch pathway or decreasing the expression of microRNA-320. Edaravone obstructed pulmonary fibrosis in a rat model of LPS-induced acute respiratory distress syndrome through inactivation of oxidative stress and transforming growth factor-β1/Smad3 signaling pathway [30]. Edaravone also alleviated experimental asthma through anti-inflammatory and antioxidative activities, which was associated with the activation of Keap1/Nrf2 pathway and heme oxygenase-1 [31]. In this study, edaravone treatment improved hemodynamics and reduced pathological changes, vascular remodeling, RV hypertrophy, cell apoptosis, oxidative stress, and α-SMA expression in the lungs of HPH mice. The expression of TNF-α and IL-6 in the serum and lungs of HPH mice also decreased after edaravone treatment. We used the STITCH website to predict the target proteins of edaravone and found there was an interaction of edaravone with NOS3.

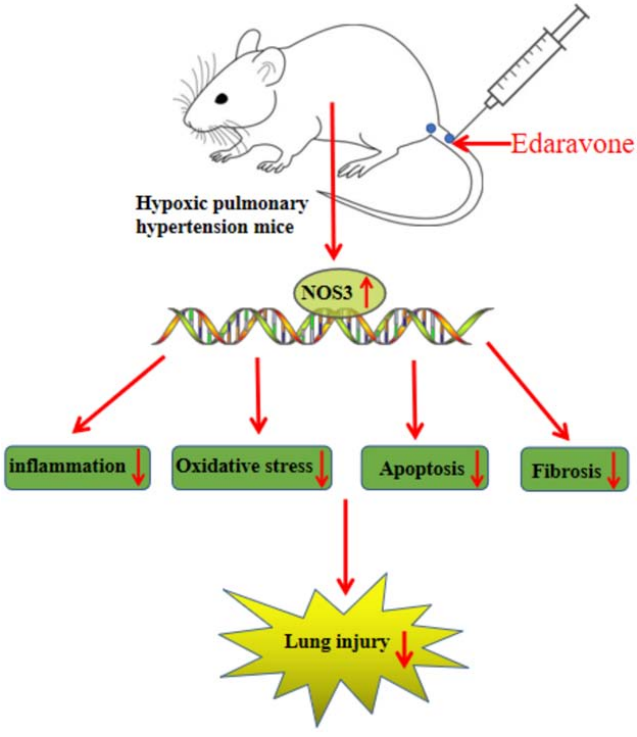


**Fig. 5. Edaravone reduces pulmonary oxidative stress, inflammation, fibrosis, and apoptosis in mice with hypoxic pulmonary hypertension by increasing the expression of NOS3.** NOS3, nitric oxide synthase 3.

Interestingly, the expression of NOS3 was increased by edaravone in the lungs of HPH mice.

NOS3 is responsible for the generation of the vast majority of NO in the endothelium and therefore controls vascular homeostasis [32]. Polymorphisms in NOS3 gene are associated with the risks of many diseases such as preeclampsia, cerebral aneurysm, migraine, acute ischemic stroke, and coronary heart disease in specific populations [33-37]. NOS3 plays a significant role in maintaining pulmonary function under normal conditions. A deficiency of NOS3 increased inflammatory responses and intensified intestinal and lung injuries post necrotizing enterocolitis [38]. Transplantation of endothelial progenitor cells reduced inflammation and pulmonary apoptosis during lung ischemia-reperfusion injury by upregulating NOS3 [39]. Many studies have shown that NOS3 could be targeted to suppress pulmonary hypertension. For example, administration of selenium by amorphous nanoparticle delivery prevented pulmonary arterial hypertension in mice through induction of tetrahydrobiopterin (BH4) salvage pathway and NOS3 recoupling [40]. Transplantation of bone marrow cells with NOS3-deficient genotypes exacerbated HPH through immune and inflammatory mechanisms [41]. C1q/TNF-related protein-9 relieved HPH by promoting the phosphorylation of AMPK and NOS3 in pulmonary microvascular endothelial cells [42]. Consistent with the previous findings, our results suggested that NOS3 was downregulated in the lungs of HPH mice. Simultaneous administration of the NOS inhibitor L-NMMA offset the lung protective effects of edaravone in HPH mice.

In summary, edaravone might impede HPH by increasing the expression of NOS3 (Fig. 5). This study first shows the antihypertensive effects of edaravone in lungs under hypoxic conditions. Deep research can be carried out to validate the therapeutic effects of edaravone in human body and broaden the approaches for managing HPH.

## FUNDING

Thanks for the grant from the Hainan Provincial Health Commission (Grant No. 19A200033).

## ACKNOWLEDGEMENTS

None.

## CONFLICTS OF INTEREST

The authors declare no conflicts of interest.

## REFERENCES

1. Mandras SA, Mehta HS, Vaidya A. Pulmonary hypertension: a brief guide for clinicians. *Mayo Clin Proc.* 2020;95:1978-1988.
2. Hoeper MM, Humbert M, Souza R, Idrees M, Kawut SM, Sliwa-Hahnle K, Jing ZC, Gibbs JS. A global view of pulmonary hypertension. *Lancet Respir Med.* 2016;4:306-322.
3. Gassmann M, Cowburn A, Gu H, Li J, Rodriguez M, Babicheva A, Jain PP, Xiong M, Gassmann NN, Yuan JX, Wilkins MR, Zhao L. Hypoxia-induced pulmonary hypertension-Utilizing experiments of nature. *Br J Pharmacol.* 2021;178:121-131.
4. Jaiswal MK. Riluzole and edaravone: a tale of two amyotrophic lateral sclerosis drugs. *Med Res Rev.* 2019;39:733-748.
5. Yoshino H. Edaravone for the treatment of amyotrophic lateral sclerosis. *Expert Rev Neurother.* 2019;19:185-193.
6. Tokumaru O, Shuto Y, Ogata K, Kamibayashi M, Bacal K, Takei H, Yokoi I, Kitano T. Dose-dependency of multiple free radical-scavenging activity of edaravone. *J Surg Res.* 2018;228:147-153.
7. Tajima S, Soda M, Bando M, Enomoto M, Yamasawa H, Ohno S, Takada T, Suzuki E, Gejyo F, Sugiyama Y. Preventive effects of edaravone, a free radical scavenger, on lipopolysaccharide-induced lung injury in mice. *Respirology.* 2008;13:646-653.
8. Yamaguchi S, Hussein MH, Daoud GA, Goto T, Kato S, Kakita H, Mizuno H, Ito T, Fukuda S, Kato I, Suzuki S, Hashimoto T, Togari H. Edaravone, a hydroxyl radical scavenger, ameliorates the severity of pulmonary hypertension in a porcine model of neonatal sepsis. *Tohoku J Exp Med.* 2011;223:235-241.
9. Król M, Kepinska M. Human nitric oxide synthase-its functions, polymorphisms, and inhibitors in the context of inflammation, diabetes and cardiovascular diseases. *Int J Mol Sci.* 2020;22:56.
10. Fish JE, Marsden PA. Endothelial nitric oxide synthase: insight into cell-specific gene regulation in the vascular endothelium. *Cell Mol Life Sci.* 2006;63:144-162.
11. Tejero J, Shiva S, Gladwin MT. Sources of vascular nitric oxide and reactive oxygen species and their regulation. *Physiol Rev.* 2019;99:311-379.
12. Lázár Z, Mészáros M, Bikov A. The nitric oxide pathway in pulmonary arterial hypertension: pathomechanism, biomarkers and drug targets. *Curr Med Chem.* 2020;27:7168-7188.
13. Chalupsky K, Kračun D, Kanchev I, Bertram K, Görlach A. Folic acid promotes recycling of tetrahydrobiopterin and protects against hypoxia-induced pulmonary hypertension by recoupling endothelial nitric oxide synthase. *Antioxid Redox Signal.* 2015;23:1076-1091.
14. Eddahibi S, Hanoun N, Lanfumey L, Lesch KP, Raffestin B, Hamon M, Adnot S. Attenuated hypoxic pulmonary hypertension in mice lacking the 5-hydroxytryptamine transporter gene. *J Clin Invest.* 2000;105:1555-1562.
15. Dias MB, Almeida MC, Carnio EC, Branco LG. Role of nitric oxide in tolerance to lipopolysaccharide in mice. *J Appl Physiol (1985).* 2005;98:1322-1327.
16. Soejima M, Koda Y. TaqMan-based real-time PCR for genotyping common polymorphisms of haptoglobin (HP1 and HP2). *Clin Chem.* 2008;54:1908-1913.
17. Hoeper MM, Ghofrani HA, Grünig E, Klose H, Olschewski H, Rosenkranz S. Pulmonary hypertension. *Dtsch Arztebl Int.* 2017;114:73-84.
18. Hu CJ, Poth JM, Zhang H, Flockton A, Laux A, Kumar S, McKeon

B, Mouradian G, Li M, Riddle S, Pugliese SC, Brown RD, Wallace EM, Graham BB, Frid MG, Stenmark KR. Suppression of HIF2 signalling attenuates the initiation of hypoxia-induced pulmonary hypertension. *Eur Respir J.* 2019;54:1900378.
19. Ahmadinejad F, Geir Møller S, Hashemzadeh-Chaleshtori M, Bidkhori G, Jami MS. Molecular mechanisms behind free radical scavengers function against oxidative stress. *Antioxidants (Basel).* 2017;6:51.
20. Bao Q, Hu P, Xu Y, Cheng T, Wei C, Pan L, Shi J. Simultaneous blood-brain barrier crossing and protection for stroke treatment based on edaravone-loaded ceria nanoparticles. *ACS Nano.* 2018;12:6794-6805.
21. Ishii H, Petrenko AB, Sasaki M, Satoh Y, Kamiya Y, Tobita T, Furutani K, Matsuhashi M, Kohno T, Baba H. Free radical scavenger edaravone produces robust neuroprotection in a rat model of spinal cord injury. *Brain Res.* 2018;1682:24-35.
22. Koike N, Sasaki A, Murakami T, Suzuki K. Effect of edaravone against cisplatin-induced chronic renal injury. *Drug Chem Toxicol.* 2021;44:437-446.
23. Masuda T, Shimazawa M, Hara H. Retinal diseases associated with oxidative stress and the effects of a free radical scavenger (edaravone). *Oxid Med Cell Longev.* 2017;2017:9208489.
24. Song Y, Bei Y, Xiao Y, Tong HD, Wu XQ, Chen MT. Edaravone, a free radical scavenger, protects neuronal cells' mitochondria from ischemia by inactivating another new critical factor of the 5-lipoxygenase pathway affecting the arachidonic acid metabolism. *Brain Res.* 2018;1690:96-104.
25. Kassab AA, Aboregela AM, Shalaby AM. Edaravone attenuates lung injury in a hind limb ischemia-reperfusion rat model: a histological, immunohistochemical and biochemical study. *Ann Anat.* 2020;228:151433.
26. Han CH, Guan ZB, Zhang PX, Fang HL, Li L, Zhang HM, Zhou FJ, Mao YF, Liu WW. Oxidative stress induced necroptosis activation is involved in the pathogenesis of hyperoxic acute lung injury. *Biochem Biophys Res Commun.* 2018;495:2178-2183.
27. Guo H, Yang R, He J, Chen K, Yang W, Liu J, Xiao K, Li H. Edaravone combined with dexamethasone exhibits synergic effects on attenuating smoke-induced inhalation lung injury in rats. *Biomed Pharmacother.* 2021;141:111894.
28. Xiao C, Du M, Liu Y, Yu Y, Yang J. Edaravone attenuates smoke inhalation injury in rats by the Notch pathway. *Am J Transl Res.* 2021;13:4712-4718.
29. Xiao C, Yu Y, Liu Y, Yang J. Aerosol inhalation of edaravone can improve inflammation, oxidative stress and pulmonary function of rats with smoke inhalation injury by down-regulating miR-320. *Am J Transl Res.* 2021;13:2563-2570.
30. Wang X, Lai R, Su X, Chen G, Liang Z. Edaravone attenuates lipopolysaccharide-induced acute respiratory distress syndrome associated early pulmonary fibrosis via amelioration of oxidative stress and transforming growth factor-β1/Smad3 signaling. *Biochem Biophys Res Commun.* 2018;495:706-712.
31. Pan Y, Li W, Feng Y, Xu J, Cao H. Edaravone attenuates experimental asthma in mice through induction of HO-1 and the Keap1/Nrf2 pathway. *Exp Ther Med.* 2020;19:1407-1416.
32. Cotta Filho CK, Oliveira-Paula GH, Rondon Pereira VC, Lacchini R. Clinically relevant endothelial nitric oxide synthase polymorphisms and their impact on drug response. *Expert Opin Drug Metab Toxicol.* 2020;16:927-951.
33. Abbasi H, Dastgheib SA, Hadadan A, Karimi-Zarchi M, Javaheri A, Meibodi B, Zanbagh L, Tabatabaei RS, Neamatzadeh H. Association of endothelial nitric oxide synthase 894G>T polymorphism with preeclampsia risk: a systematic review and meta-analysis based on 35 studies. *Fetal Pediatr Pathol.* 2021;40:455-470.
34. Chen XJ, Qiu CG, Kong XD, Ren SM, Dong JZ, Gu HP, Chen YW, Tao HL, Sarbesh J. The association between an endothelial nitric oxide synthase gene polymorphism and coronary heart disease in young people and the underlying mechanism. *Mol Med Rep.* 2018;17:3928-3934.
35. Dong H, Wang ZH, Dong B, Hu YN, Zhao HY. Endothelial nitric oxide synthase (-786T>C) polymorphism and migraine susceptibility: a meta-analysis. *Medicine (Baltimore).* 2018;97:e12241.
36. Paschoal EHA, Yamaki VN, Teixeira RKC, Paschoal Junior FM, Jong-A-Liem GS, Teixeira MJ, Yamada ES, Ribeiro-Dos-Santos Â, Bor-Seng-Shu E. Relationship between endothelial nitric oxide synthase (eNOS) and natural history of intracranial aneurysms: meta-analysis. *Neurosurg Rev.* 2018;41:87-94.
37. Saluja A, Saraswathy KN, Thakur S, Margekar S, Goyal A, Dhamija RK. Endothelial nitric oxide synthase (Glu298Asp) polymorphism is associated significantly with ischemic stroke presenting with seizures and altered sensorium. *Neurol India.* 2021;69:686-691.
38. Drucker NA, Jensen AR, Te Winkel JP, Ferkowicz MJ, Markel TA. Loss of endothelial nitric oxide synthase exacerbates intestinal and lung injury in experimental necrotizing enterocolitis. *J Pediatr Surg.* 2018;53:1208-1214.
39. Gao W, Jiang T, Liu YH, Ding WG, Guo CC, Cui XG. Endothelial progenitor cells attenuate the lung ischemia/reperfusion injury following lung transplantation via the endothelial nitric oxide synthase pathway. *J Thorac Cardiovasc Surg.* 2019;157:803-814.
40. Zhu ML, Gao ZT, Lu JX, Wang Y, Wang G, Zhu TT, Li P, Liu C, Wang SX, Yang L. Amorphous nano-selenium quantum dots prevent pulmonary arterial hypertension through recoupling endothelial nitric oxide synthase. *Aging (Albany NY).* 2020;13:3368-3385.
41. Ogoshi T, Tsutsui M, Kido T, Sakanashi M, Naito K, Oda K, Ishimoto H, Yamada S, Wang KY, Toyohira Y, Izumi H, Masuzaki H, Shimokawa H, Yanagihara N, Yatera K, Mukae H. Protective role of myelocytic nitric oxide synthases against hypoxic pulmonary hypertension in mice. *Am J Respir Crit Care Med*. 2018;198:232-244.
42. Jin Q, Su H, Yang R, Tan Y, Li B, Yi W, Dong Q, Zhang H, Xing W, Sun X. C1q/TNF-related protein-9 ameliorates hypoxia-induced pulmonary hypertension by regulating secretion of endothelin-1 and nitric oxide mediated by AMPK in rats. *Sci Rep.* 2021;11:11372.